

## From criticality to supercooling in expanding hot nuclear matter: Possible explanation of low- $\tau$ puzzle

Larissa V. Bravina and Eugene E. Zabrodin

*Department of Physics, University of Bergen, Allègaten 55, N-5007 Bergen, Norway  
and Institute for Nuclear Physics, Moscow State University, 119899 Moscow, Russia*

(Received 14 February 1996)

A model of an expanding hot nuclear matter is discussed. A Fokker-Planck equation is used to describe the conversion of the gaseous phase into the liquid phase. It is shown that the apparent exponent  $\tau_{\text{eff}}$  entering the power-law fit to charge fragment distribution  $\sigma(Z) \propto Z^{-\tau_{\text{eff}}}$  differs considerably from the critical exponent  $\tau$ . If the nuclear matter is strongly supercooled,  $\tau_{\text{eff}}$  should be small both for small and for large systems. This fact may serve as a possible explanation of the low values of  $\tau_{\text{eff}}$ , obtained recently at Michigan State University. [S0556-2813(96)50608-4]

PACS number(s): 25.70.Pq, 21.65.+f, 24.60.Ky

A large amount of data obtained in nuclear reactions at intermediate energies has inspired a great deal of theoretical efforts to describe the multifragmentation phenomenon (see, e.g., [1–21], and references therein). The possibility to fit the yield of light fragments with the simple power-law dependence

$$Y(A) = Y_0 A^{-\tau_{\text{eff}}}, \quad (1)$$

first demonstrated by the Purdue-Fermilab collaboration [1], has attracted attention to critical phenomena connected with the liquid-gas phase transition in nuclear matter. Indeed, the distribution of clusters of the new phase should obey a universal power law near the critical temperature, according to Fisher's theory of condensation [22]. On the other hand, the apparent exponent  $\tau_{\text{eff}}$  entering Eq. (1), was found to lie far from the range of the critical exponent  $\tau = 2.2 \pm 0.1$ . To avoid the ambiguity it was pointed out [4–6] that the expanding nuclear matter cannot hit the critical point accidentally in different reactions at any energies. Modification of the expansion scenario concerns the quenching of the fireball into the metastable or even unstable regions where the first-order phase transition should take place. Therefore, one has to take into account the bulk and surface energies associated with the creation of a droplet of the new phase. A new approximation to the fragment distribution was proposed as

$$Y(A) = Y_0 A^{-\tau} \exp(aA - bA^{2/3}), \quad (2)$$

where  $a$  and  $b$  are bulk and surface energies, and  $\tau$  is the critical exponent. This expression is often used to fit the fragment distribution according to

$$Y(A) = Y_0 A^{-\tau} X^A Y^{A^{2/3}}, \quad (3)$$

containing  $Y_0$ ,  $X$ , and  $Y$  as fitting parameters. The apparent exponent  $\tau_{\text{eff}}$  is expected to reach its minimal value at the critical point, where Eq. (2) is transformed into Eq. (1), and, therefore,  $\tau_{\text{eff}} \geq \tau$ . On the contrary, the experimental data on nuclear fragmentation in  $^{40}\text{Ar} + ^{45}\text{Sc}$  central collisions [23,24] show that the minimal value of  $\tau_{\text{eff}}$  may be about 1.2. One of the possible explanations of the disagreement is connected with the finiteness of the system of colliding nuclei.

Calculations performed by a bond-breaking percolation model [24] demonstrate the saturation in an increase of the critical exponent with the enlargement of lattice size. According to this model, finite size corrections to  $\tau_{\text{eff}}$  are negligibly small for a system with 200 or more nucleons. On the other hand, the extremely low value of the apparent exponent  $\tau_{\text{eff}} \approx 1.22$  was measured recently in central Au+Au collisions at 35A MeV [25]. Neither the existence of a nonequilibrium mixture of fragments and a supersaturated nucleonic gas at freeze out [11], nor the noncompact bubblelike decay configurations [17,18] can explain such low values of the apparent exponents. Finally, lattice gas model calculations mapped to molecular dynamics calculations with the inclusion of the Coulomb interactions [21] can force the calculated values for  $\tau_{\text{eff}}$  to reach  $\tau_{\text{eff}} \approx 1.3$  at very low temperature  $T \approx 0.8 - 1.0$  MeV [25]. It means that to hit  $\tau_{\text{eff}} \approx 1.2$  the system should disintegrate when it is almost in a ground state, which is unlikely to be true.

As is shown below, experimental data can be described in a consistent manner within the general theory of a first-order phase transition. In the present paper we continue to develop the approach to the liquid-gas phase transition in nuclear matter, based on the results obtained within the general theory of nucleation [26], and then applied to nuclear fragmentation [27,28]. Keeping the aforementioned evolution of the long-lived fireball as a working hypothesis, our scenario presumes the kinetic description of cluster formation during the condensation of a gas of nucleons. We start from the free energy, associated with the forming in the initially homogeneous gas of a spherical droplet of mass  $A$  and radius  $R = r_0 A^{1/3}$ , where  $r_0$  is the nucleon radius. The change in the Helmholtz free energy of the system due to the droplet formation is given by the Myers-Swiatecki formula [29] generalized to the case of nonzero temperature [13]

$$\Delta F = -\frac{4\pi}{3} R^3 \Delta p + 4\pi R^2 \sigma + \tau T \ln A + \frac{3}{5} \frac{Z^2 e^2}{R} \left( 1 - \frac{R}{R_{\text{cell}}} \right) \quad (4)$$

containing the bulk, surface, curvature (or Fisher), and Coulomb terms, the last one calculated within the Wigner-Seitz approximation [7]. Here  $\Delta p$  is the difference between the

pressure inside and outside the droplet,  $\sigma$  is the surface tension,  $T$  is the temperature of the system,  $Z$  is the droplet charge, and  $R_{\text{cell}}$  is the radius of the cell on which the droplet is formed. If  $(\rho_L, Z, A)$  and  $(\rho, Z_0, A_0)$  are the baryon density, charge, and mass inside the droplet and inside the cell, respectively, one may write [7]

$$\delta = \frac{R}{R_{\text{cell}}} = \left( \frac{(Z_0/A_0)\rho}{(Z/A)\rho_L} \right)^{1/3}. \quad (5)$$

In our analysis  $\rho$  and  $\rho_L$  are determined as the endpoints of the Maxwell construction in a pressure versus volume per particle plot of the nuclear equation of state [13]. The associated free energy  $\Delta F$  reaches its maximal value at the critical radius  $R_c$  where  $\partial[\Delta F(R)]/\partial R = 0$ . The droplets of critical radii are in metastable equilibrium, droplets smaller than that of critical size are shrinking, and droplets larger than the critical droplet are growing. Following the classical nucleation theory [30,31] we consider the evaporation-condensation mechanism as an underlying physical process by which the nuclear droplets can grow or dissolve. Then, the droplet distribution obeys a Fokker-Planck equation

$$\frac{\partial f}{\partial t} = B \frac{\partial^2 f}{\partial^2 R} - A \frac{\partial f}{\partial R}, \quad (6)$$

containing the size drift and size diffusion coefficients  $A$  and  $B$ . Using the mathematical formalism formulated in details in [26–28] one may find the steady-state solution of Eq. (6) for a given free energy  $\Delta F$  associated with a droplet formation. The principal result is that the equilibrium distribution function (EDF) given, e.g., by Eq. (2) or, generally, by the canonical distribution

$$f(R) = I_0 \exp\left(-\frac{\Delta F}{T}\right), \quad (7)$$

which cannot describe the dynamics of a first-order phase transition [31], is replaced by the nonequilibrium, steady-

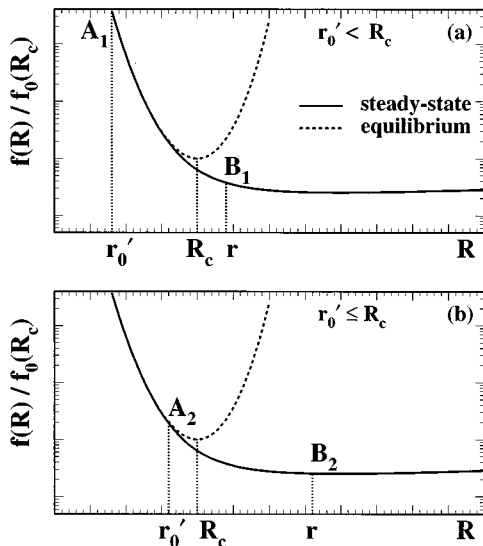


FIG. 1. Schematic plot of equilibrium and steady-state distribution functions. See text for the details.

state distribution function (SDF) corresponding to a continuous conversion of the phase  $I$  into the phase  $II$ .

In terms of the dimensionless parameters  $\lambda = (4\pi\sigma/T)^{1/2}R_c$ ,  $y = R/R_c$ , and  $\gamma = 3e^2R_c^5/5T\tau_0^6$  the SDF of droplets reads

$$f(R) = f_0(R_c) y^{-3\tau} \exp\left(\frac{\gamma\delta}{4} - \frac{\gamma}{6} - \tau + \frac{1}{3}\lambda^2\right) \times \exp\left[\frac{\gamma\delta}{4}y^6 - \frac{\gamma}{4}y^5 + \left(-\frac{\gamma\delta}{2} + \frac{5}{12}\gamma + \frac{2}{3}\lambda^2 + \tau\right)y^3 - \lambda^2y^2\right] \frac{\text{Int}[y, \infty]}{\text{Int}[0, \infty]}, \quad (8)$$

where

$$\text{Int}[a, b] = \int_a^b z^{3\tau+1} \left[ \left( \frac{3}{2} \gamma \delta z^3 + 3\tau \right) (z^2 + z + 1) - \frac{5}{4} \gamma z^3 (z + 1) + 2\lambda^2 z^2 \right] \exp\left[ -\frac{\gamma\delta}{4}z^6 + \frac{\gamma}{4}z^5 - \left( -\frac{\gamma\delta}{2} + \frac{5}{12}\gamma + \frac{2}{3}\lambda^2 + \tau \right) z^3 + \lambda^2 z^2 \right] dz, \quad (9)$$

$$f_0(R_c) = I_0 \exp\left(-\frac{\Delta F(R_c)}{T}\right), \quad (10)$$

and  $I_0$  is a preexponential factor.

The EDF and SDF are shown schematically in Fig. 1. First, it should be noted that the SDF has no distinct minimum at  $R \geq R_c$ , compared to the EDF. Then, let  $r'_0$  be the radius of the smallest fragment from the range of intermediate mass fragments. It is worthwhile to note how the ratio  $r'_0/R_c$  influences the results. When the system approaches the critical temperature, the critical radius goes to infinity, and one should find the simple power-law dependence  $A^{-\tau}$  for the yield of fragments. But, if the system is supercooled, the value of the critical radius falls quickly. When the critical

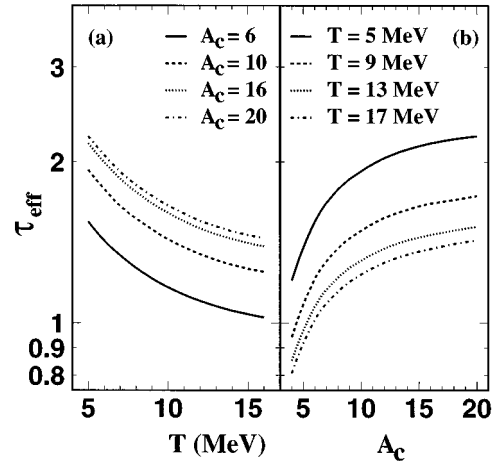


FIG. 2. (a) Apparent exponent  $\tau_{\text{eff}}$  as a function of temperature of the nuclear system for different sizes of critical nuclei  $A_c$ . (b) Apparent exponent  $\tau_{\text{eff}}$  as a function of  $A_c$  at different temperatures.

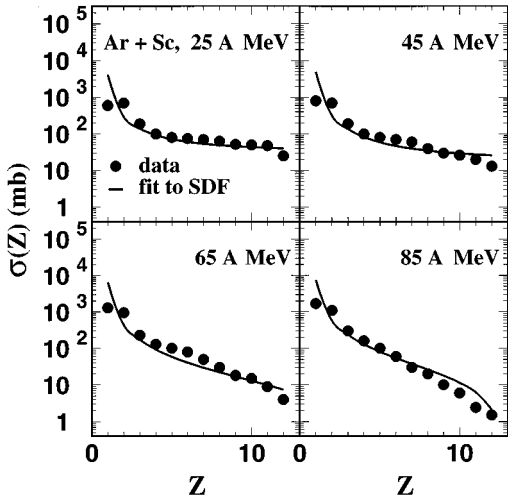


FIG. 3. Charge distributions of fragments (full circles) measured in the  $^{40}\text{Ar}+^{45}\text{Sc}$  central collisions at 25A to 85A MeV. Data are taken from [24]. Solid lines correspond to the fit to Eq. (8).

radius is twice as large as  $r'_0$ , the slope of the SDF remains steep [part  $A_1B_1$ , Fig. 1(a)]. Finally, if the critical radius is about  $1.5 r'_0$  or less (strong supercooling), the distribution of the fragments becomes rather flat [part  $A_2B_2$ , Fig. 1(b)]. One has to bear this scenario in mind because of the restriction on minimal charge of the intermediate mass fragments to  $Z_{\min} \geq 3$ .

To study the dependence of  $\tau_{\text{eff}}$  on the size of a critical cluster at different temperatures, the fragment distributions were calculated according to Eqs. (8) and (9). Parameters entering these equations were chosen as follows: critical temperature,  $T_c = 20.69$  MeV [4], surface tension  $\sigma(T) = \sigma_0[(T_c^2 - T^2)/(T_c^2 + T^2)]^{5/4}$ ,  $\sigma_0 = 18$  MeV [7], and nucleon radius  $r_0 = 1.17$  fm. The set of effective exponents as a function of temperature and critical size of the fragments is displayed in Fig. 2. One can see that  $\tau_{\text{eff}}$  may be about unit or even less, while the critical exponent  $\tau$  is always 2.2. This statement should be valid both for light and heavy systems, not only for the light ones as predicted by the percolation model calculations.

The last problem to discuss before the comparison with the experimental data is the long tail of the SDF. Let us turn to Eq. (9). The sign of the polynomial in the integrand may be changed from plus to minus in the interval  $0 \leq y \leq 1$ , if the temperature is high enough to maintain large values of the critical radius and, therefore,  $\gamma$ . It means that the fragment distribution will have a significant gap between the light and heavy fragments instead of a plateau in the intermediate mass region. Furthermore, the yield of the light fragments

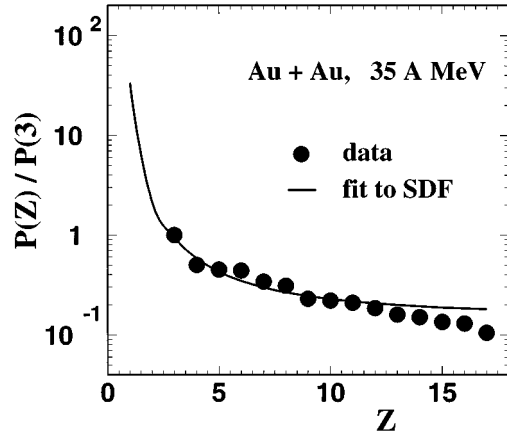


FIG. 4. Relative elemental yield (full circles) measured in the Au+Au central collisions at 35A MeV. Data are taken from [25]. Solid line corresponds to the fit to Eq. (8).

falls almost exponentially in the last case. This fact may be considered as a consequence of the destabilizing long-range Coulomb forces at relatively high temperatures.

Charge distributions of fragments measured in central  $^{40}\text{Ar}+^{45}\text{Sc}$  collisions at 25A to 85A MeV [24] and in central Au+Au interactions at 35A MeV at Michigan State University [25] are presented in Figs. 3, 4. Curves plotted onto the experimental data are the fits to the SDF, given by Eq. (8). Parameters of the fit are listed in Table I. The rise of the slope exponent and transformation of the shape of fragment distribution from the power law to the almost exponential one may be explained by the increase of the break-up temperature of the system from 6.5 MeV to 10.2 MeV due to the rise of initial excitation energy. The break-up temperature and the mass of the critical cluster, obtained for the gold-on-gold reaction, fit well to the same parameters, obtained for the Ar+Sc collisions. To investigate the role of the finite size effects it would be nice to perform the experiment with heavy ions at the same excitation energies as in the Ar+Sc experiment.

The results of this paper may be summarized as follows. We propose a model of an expanding fireball that undergoes a first-order phase transition. A Fokker-Planck equation is used to describe the conversion of the gaseous phase into the liquid phase. The fireball disintegrates below some critical density, say,  $0.3 \rho_0$ , where  $\rho_0$  is the normal nuclear density. The higher the excitation energy of the initial system, the higher the break-up temperature of the expanding fireball should be, and vice versa. Coulomb forces are responsible for the almost exponential falloff of the fragment distribution at the relatively high temperatures corresponding to the high

TABLE I. The results of the fit of experimental  $Z$  distributions shown in Figs. 3, 4 to the steady-state distribution function. Of each pair of numbers, the upper one denotes the temperature and the lower one denotes the mass of the critical nucleus.

	$^{40}\text{Ar}+^{45}\text{Sc}$				Au+Au
	25A MeV	45A MeV	65A MeV	85A MeV	35A MeV
$T$	$6.5 \pm 0.2$	$7.5 \pm 0.2$	$9.3 \pm 0.2$	$10.2 \pm 0.2$	$6.9 \pm 0.2$
$A_c$	$9.0 \pm 0.5$	$13.0 \pm 1.0$	$49.0 \pm 2.0$	$55.5 \pm 2.0$	$11.0 \pm 0.5$

excitation energies. At lower temperatures the radius of the critical clusters diminishes quickly, and the fragment distributions can be fairly well approximated with the simple power law. The ratio of the radius of the smallest cluster from the intermediate mass range to the radius of a critical cluster in the system  $r'_0/R_c$  plays an essential role for the shape of the yield curve of fragments. If the system is supercooled, the fragment distribution becomes quite flat at  $Z \geq 3$  chosen for the experimental selection of the intermediate mass fragments, and the effective exponent of the power-law fit may be very small both for small and large systems. This is the principle difference between the approach pro-

posed and the percolation model. We do not agree that the flattening of the fragment distributions may be explained by a Coulomb-driven multifragment decay at extremely low temperatures. Although the experimental data appear to favor the supercooling in nuclear matter, the problem deserves further investigations.

Discussions with J. P. Bondorf, L. P. Csernai, I. N. Mishustin, and V. Zelevinsky are gratefully acknowledged. We would like to thank K. Nybø for the helpful comments. We are indebted to the Department of Physics, University of Bergen for the warm and kind hospitality.

- 
- [1] J. E. Finn *et al.*, Phys. Rev. Lett. **49**, 1321 (1982); R. W. Minich *et al.*, Phys. Lett. **118B**, 458 (1982).
- [2] G. Fai and J. Randrup, Nucl. Phys. **A404**, 551 (1983).
- [3] H. R. Jaqaman, A. Z. Mekjian, and L. Zamick, Phys. Rev. C **29**, 2067 (1984).
- [4] A. L. Goodman, J. I. Kapusta, and A. Z. Mekjian, Phys. Rev. C **30**, 851 (1984).
- [5] A. D. Panagiotou, M. W. Curtin, H. Toki, D. K. Scott, and P. J. Siemens, Phys. Rev. Lett. **52**, 496 (1984); A. D. Panagiotou, M. W. Curtin, and D. K. Scott, Phys. Rev. C **31**, 55 (1985).
- [6] L. P. Csernai and J. I. Kapusta, Phys. Rep. **131**, 223 (1986).
- [7] J. P. Bondorf, A. S. Botvina, A. S. Iljinov, I. N. Mishustin, and K. Sneppen, Phys. Rep. **257**, 133 (1995); J. P. Bondorf, R. Donangelo, I. N. Mishustin, C. J. Pethick, H. Schulz, and K. Sneppen, Nucl. Phys. **A443**, 321 (1985).
- [8] W. Bauer, U. Post, D. R. Dean, and U. Mozel, Nucl. Phys. **A452**, 699 (1986).
- [9] S. Koonin and J. Randrup, Nucl. Phys. **A474**, 173 (1987).
- [10] X. Campi, Phys. Lett. B **208**, 351 (1988).
- [11] M. Mahi *et al.*, Phys. Rev. Lett. **60**, 1936 (1988).
- [12] W. A. Friedman, Phys. Rev. Lett. **60**, 2125 (1988); Phys. Rev. C **42**, 667 (1990).
- [13] A. R. DeAngelis and A. Z. Mekjian, Phys. Rev. C **40**, 105 (1989).
- [14] H. R. Jaqaman and D. H. E. Gross, Nucl. Phys. **A524**, 321 (1991).
- [15] A. R. DeAngelis, D. H. E. Gross, and R. Heck, Nucl. Phys. **A537**, 606 (1992).
- [16] S. J. Lee and A. Z. Mekjian, Phys. Rev. C **45**, 1284 (1992).
- [17] L. Phair, W. Bauer, and C. K. Gelbke, Phys. Lett. B **314**, 271 (1993).
- [18] D. H. E. Gross and K. Sneppen, Nucl. Phys. **A567**, 317 (1994).
- [19] K. C. Chase and A. Z. Mekjian, Phys. Rev. C **49**, 2164 (1994).
- [20] J. Pan and S. Das Gupta, Phys. Rev. C **51**, 1384 (1995); Phys. Lett. B **344**, 29 (1995).
- [21] S. Das Gupta and J. Pan, Phys. Rev. C **53**, 1319 (1996).
- [22] M. E. Fisher, Physics (Long Island City, N.Y.) **3**, 255 (1967).
- [23] T. Li *et al.*, Phys. Rev. Lett. **70**, 1924 (1993).
- [24] T. Li *et al.*, Phys. Rev. C **49**, 1630 (1994).
- [25] M. D'Agostino *et al.*, Phys. Rev. Lett. **75**, 4373 (1995).
- [26] L. V. Bravina and E. E. Zabrodin, Phys. Lett. A **202**, 61 (1995).
- [27] E. E. Zabrodin, Phys. Rev. C **52**, 2608 (1995).
- [28] L. V. Bravina and E. E. Zabrodin, Phys. Rev. C (submitted).
- [29] W. Myers and V. Swiatecki, Ann. Phys. (N.Y.) **55**, 395 (1969).
- [30] J. Frenkel, *Kinetic Theory of Liquids* (Dover, New York, 1955), Chap. 7.
- [31] E. M. Lifshitz and L. P. Pitaevskii, *Physical Kinetics* (Pergamon, Oxford, 1981), Chap. 12.